



Short communication

Accuracy of single-plane fluoroscopy in determining relative position and orientation of total knee replacement components

Stacey Acker^{a,*}, Rebecca Li^a, Heather Murray^a, Paul St. John^b, Scott Banks^{c,d}, Shang Mu^{c,d}, Urs Wyss^e, Kevin Deluzio^a^a Department of Mechanical and Materials Engineering, Queen's University, Kingston, Ontario, Canada K7L 3N6^b Human Mobility Research Centre, Kingston General Hospital, Kingston, Ontario, Canada^c Mechanical and Aerospace Engineering, Canada, University of Florida, Gainesville, Florida, USA^d Orthopaedics and Rehabilitation, University of Florida, Gainesville, Florida, USA^e Department of Mechanical and Manufacturing Engineering, University of Manitoba, Winnipeg, Manitoba, Canada

ARTICLE INFO

Article history:

Accepted 25 October 2010

Keywords:

Knee
Joint kinematics
Fluoroscopy
Accuracy

ABSTRACT

The accuracy of estimating the relative pose between knee replacement components, in terms of clinical motion, is important in the study of knee joint kinematics. The objective of this study was to determine the accuracy of the single-plane fluoroscopy method in calculating the relative pose between the femoral component and the tibial component, along knee motion axes, while the components were in motion relative to one another. The kinematics of total knee replacement components were determined in vitro using two simultaneous methods: single-plane fluoroscopic shape matching and an optoelectronic motion tracking system. The largest mean differences in relative pose between the two methods for any testing condition were 2.1°, 0.3°, and 1.1° in extension, abduction, and internal rotation respectively, and 1.3, 0.9, and 1.9 mm in anterior, distal, and lateral translations, respectively. For the optimized position of the components during dynamic trials, the limits of agreement, between which 95% of differences can be expected to fall, were –2.9 to 4.5° in flexion, –0.9 to 1.5° in abduction, –2.4 to 2.1° in external rotation, –2.0 to 3.9 mm in anterior-posterior translation, –2.2 to 0.4 mm in distal-proximal translation and –7.2 to 8.6 mm in medial-lateral translation. These mean accuracy values and limits of agreement can be used to determine whether the shape-matching approach using single-plane fluoroscopic images is sufficiently accurate for an intended motion tracking application.

© 2010 Elsevier Ltd. All rights reserved.

1. Introduction

Single-plane fluoroscopy has been used extensively to track the motion of total knee replacements. Its accuracy has been investigated previously (Banks and Hodge, 1996; Mahfouz et al., 2003; Yamazaki et al., 2004; Zuffi et al., 1999). However, the previous studies have some limitations. Accuracies of less than 1.1 mm and 1° have been reported, but these values are for estimating the pose of a single component in a given coordinate system. To our knowledge, no single study has reported the accuracy of a fluoroscopic approach specifically in determining the *relative pose* between the femur and tibia component along knee motion axes, while the components were in motion relative to one another (simulating an actual motion tracking application).

If the fluoroscopic method is to be applied in the study of knee kinematics or in the validation of other motion tracking systems in tracking knee kinematics, an estimate of the accuracy of the fluoroscopic approach in determining relative knee joint

kinematics must be determined in dynamic applications and in terms of clinically relevant quantities. The objective of this study was to determine the accuracy of knee joint kinematics calculated using the fluoroscopic shape matching approach by comparing it to optoelectronic motion tracking.

2. Methods

Cruciate-substituting mobile bearing total knee replacement components (Innex, Zimmer GmbH, Winterthur, Switzerland) were implanted into femur and tibia Sawbones (Pacific Research Laboratories Inc., Washington, USA). Elastics were used to attach the two Sawbones and to simulate collateral ligaments. One infrared marker set was attached to each Sawbone, forming a coordinate system that moved rigidly with the Sawbone to which it was attached (Fig. 1).

Before implantation, a probe was used to digitize features (surfaces) and registration landmarks on the exposed surface of the femoral and tibial components so that the position of the implant coordinate system could be determined after implantation when the defining features of the CAD model coordinate system were no longer accessible. Small (< 1 mm diameter) surface registration landmarks were made using a hardness tester and did not alter the silhouette of the implant. After implantation, the landmarks were digitized to create transformation matrices between the marker coordinate system and the component coordinate system. Once determined, the component pose matrices were then used to calculate the Euler

* Corresponding author. Tel.: 613 533 6737; fax: 613 533 6489.
E-mail address: acker@me.queensu.ca (S. Acker).

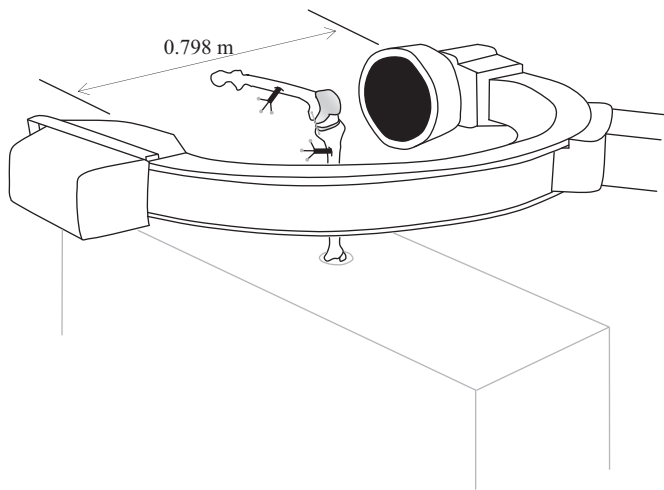


Fig. 1. Experimental set-up. Images were taken using a C-arm fluoroscope while infrared marker clusters on the tibia and femur were tracked by Optotrak Certus camera. Dynamic trials started with the knee at approximately 95° flexion. The femur was manually moved through an extension cycle to 0°.

Table 1
Static pose angles for the six static poses (as calculated from the optoelectronic motion data).

Flexion angle (degrees)	Abduction angle (degrees)	External rotation angle (degrees)
13.7	0.1	9.1
14.4	0.0	21.5
10.4	6.8	5.8
72.1	0.4	-5.3
73.8	0.1	10.4
72.4	3.9	-2.8

angles (rotation order: flexion, abduction, then external rotation) and position of the femur relative to the tibia (Grood and Suntay, 1983).

Trials were recorded simultaneously (~8 Hz) using an Optotrak Certus camera (Northern Digital Inc., Waterloo, Ontario, Canada) and an OEC 9800 C-arm fluoroscope (GE OEC Medical Systems, Salt Lake City, Utah, USA), using custom synchronization software. During static trials, the Sawbones were set in one of six static poses (Table 1) while a series of frames were recorded. Five frames were randomly selected from each static pose for a total of thirty 640 × 480 images. During five dynamic trials, the femur Sawbone was manually moved through a knee extension cycle (~95° to ~0° flexion). Tension in the simulated collateral ligaments held the femoral component against the polyethylene insert, meaning implant geometry guided the relative motion. Any abduction/adduction or external/internal rotation of the knee during the trial occurred as a natural consequence of implant geometry during flexion of the implant.

Calibration and distortion correction parameters were determined using a calibration image of radiopaque beads in known patterns (Camera Calibration Toolbox for Matlab, The Mathworks Inc., Natick, Massachusetts, USA) and were used to correct all trial images. Corrected images and CAD models were imported into an open source shape-matching software program (JointTrack, University of Florida, <http://sourceforge.net/projects/jointtrack/>). By manually changing the position and orientation of the CAD models on display, the contour of the CAD model was manually matched to the extracted contour (Canny, 1986) of the component silhouette in the fluoroscopic image (Fig. 2). After manually positioning the implant components, the poses were optimized. The automated local optimization algorithm was based on the method described by Mahfouz et al. (2003) and involves comparison of the actual X-ray image to a predicted X-ray image created based on the initial pose of the components and the known geometry and parameters of the fluoroscope. The shape match between the two images was evaluated based on a weighted combination of two metrics. The first metric was a correlation on the intensity values of the two images and the second was a correlation on the shape contours (Mahfouz et al., 2003). The edge contour correlation is weighted more heavily (weight: 2.67) than the intensity correlation (weight: 1.0). These weights were determined experimentally for best results in Mahfouz et al. (2003).

Normally, when shape matching sequential frames, the pose in the preceding frame is used to aid the operator in matching the current frame since the knee joint motion is expected to be smooth (Zuffi et al., 1999). All 176 collected dynamic trial images were matched in the order they were collected in order to simulate a typical application. The order of static images was instead randomized so that the operator had to start the matching from scratch for each frame. This assessed the repeatability with which an image from the same static trial could be re-matched. The pose matrices for each component were used to determine the pose of the femur relative to the tibia.

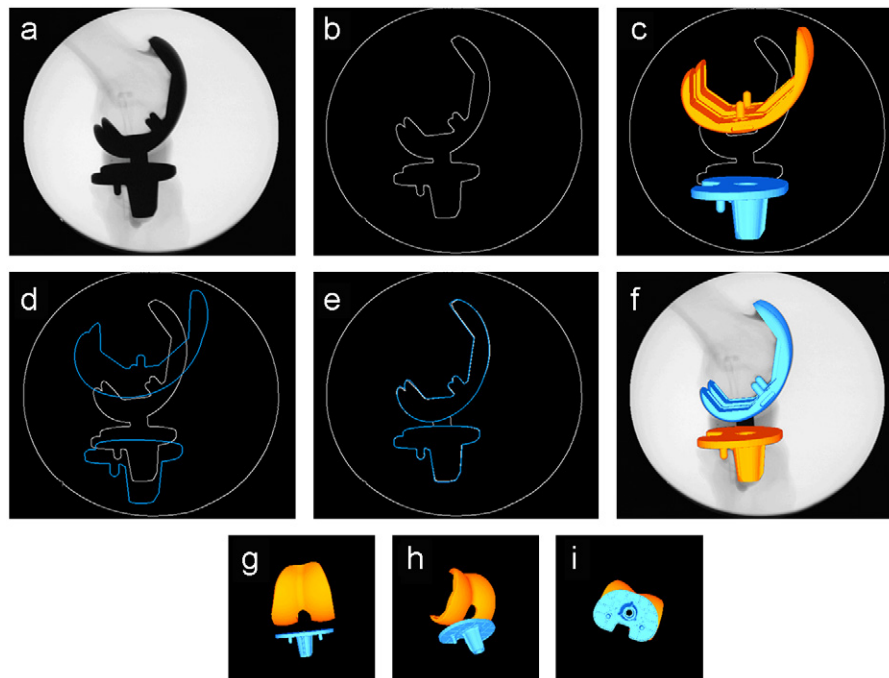


Fig. 2. Shape matching software display. (a) Original fluoroscopic image. (b) Edges extracted from the fluoroscopic image. (c) CAD models of the implants imported into the software. (d) Outline view of the implants positioned in front of image edge view. (e) The position and orientation of the CAD model has been manually manipulated so that the two shape outlines match. (f) The 3D solid model view of the implant in the matched position. (g)–(i) Free rotation views of the implant in the matched position. The software operator can freely rotate the viewing angle of the implant components. Note: Only the femoral and tibial CAD models were shape matched with the femoral and tibial silhouettes in the images. The implant was a mobile bearing design that included a post that is inserted into the tibial component. The post is visible in the fluoroscopic images as a solid silhouette between the femoral and tibial silhouettes. A CAD model of the post was not shape matched to the post silhouette.

The differences between the two methods were calculated for each data frame (30 static frames, 176 dynamic frames). The agreement between the optoelectronic and fluoroscopic results was described by the “limits of agreement” approach (Altman and Bland, 1983). This method defines an upper and lower limit, between which 95% differences between the two methods can be expected to fall. Since a single-factor ANOVA showed a trial effect, each trial was treated separately and a pooled variance was used (Bland and Altman, 1999, 2007). Hypothesis testing was used to find any significant differences between the fluoroscopic and optoelectronic results for either static or dynamic conditions, or between the static and dynamic results. *P*-values were corrected for multiple tests using a Bonferroni step-down (Holm) correction for 18 tests (6 response variables, 3 comparison tests). Statistical significance was defined by an adjusted *P*-value less than 0.05.

3. Results

All average differences (bold, Table 2) were 2.1° and 1.9 mm or under, and differences were normally distributed. The Bland–Altman plots of the dynamic trial data (Figs. 3 and 4) showed no linear trends, except in medial–lateral translation (Fig. 4c, $R^2=0.9$). The x-intercept of the trend is near zero because the optoelectronic method tracked a smaller range of medial–lateral translations (−1.3 to 1.8 mm) than the fluoroscopic method (−10.0 to 8.5 mm). When the mean of the two methods was near zero (translations from both methods were small), the methods were in better agreement. From the static trials, the standard deviations of the differences were 1.2°, 0.4°, and 1.0° in flexion, abduction, and external rotation, respectively, and 1.3, 0.8, and 4.5 mm in the anterior–posterior, distal–proximal, and medial–lateral translations, respectively. These values reflect how repeatably images from the same static trial were matched after optimization without knowledge of the preceding frame in the trial.

4. Discussion

The objective of this study was to determine the accuracy of total knee replacement kinematics determined via fluoroscopic shape matching using shape matching software and an optimization algorithm. The largest absolute mean differences in relative pose between the fluoroscopic and optoelectronic results were 2.1°, 0.3°, and 1.1° in extension, abduction, and internal rotation, respectively, and 1.3, 0.9, and 1.9 mm in anterior, distal, and lateral translations, respectively. The differences between the two methods were always significantly different from zero; however, the intended application of the knee joint kinematics data would have to be considered to determine whether or not these errors would be acceptable. This study was a pre-cursor to a study on the accuracy

Table 2

Mean differences between methods. The limits of agreement in brackets indicate the lower and upper limits between which 95% of the differences between the two methods can be expected to fall.

Difference	Static trials	Dynamic trials
Flexion*	−2.1	0.8
(degrees)	(−4.4 to 0.3)	(−2.9 to 4.5)
Abduction	0.3	0.3
(degrees)	(−0.5 to 1.1)	(−0.9 to 1.5)
External rotation*	−1.1	−0.2
(degrees)	(−3.2 to 1.0)	(−2.4 to 2.1)
Anterior–posterior	1.3	0.9
Translation (mm)	(−1.3 to 3.8)	(−2.0 to 3.9)
Distal–proximal*	−0.5	−0.9
Translation (mm)	(−2.1 to 1.2)	(−2.2 to 0.4)
Medial–lateral	1.9	0.7
Translation (mm)	(−7.2 to 10.9)	(−7.2 to 8.6)

* Significant difference between the static difference and the corresponding dynamic difference. Statistical significance was defined by an adjusted *p*-value less than 0.05.

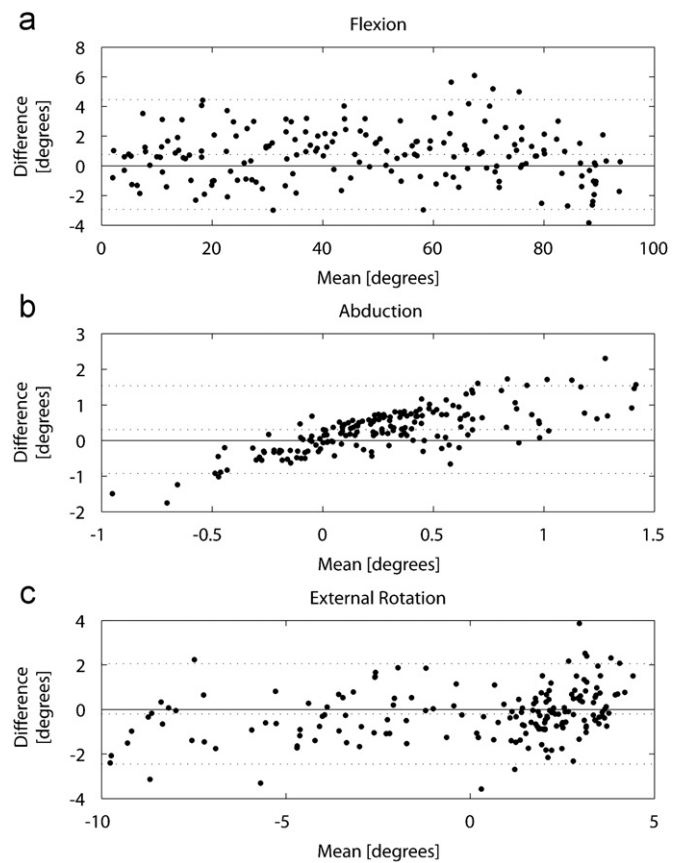


Fig. 3. Bland–Altman plots indicating the agreement between the two methods in determining relative knee joint angles during dynamic trials. For each pair of observations (one for the fluoroscopic method and one for the optoelectronic method), one point is plotted at the mean (horizontal axis) of the two observations and the difference (vertical axis) of the two observations. One Bland–Altman figure is plotted for each of the rotation axes: (a) flexion, (b) abduction, and (c) external rotation. The centre dotted line is plotted at the mean difference between the two methods. The upper and lower dotted lines are the limits of agreement, between which 95% of differences between the two methods are expected to fall.

of a skin marker motion tracking system. The accuracy of the fluoroscopic method found in this study is well below that which would be required in a comparison with skin marker systems.

Differences between the static results and the corresponding dynamic results were statistically significant in flexion, external rotation, and distal–proximal translation. With the exception of distal–proximal translation, dynamic trials had the same average results as, or better average results than, the static trials, which may be because the operator had the advantage of knowing the preceding and following frames, whereas the static images were processed in a random order.

All average errors were within 2.1° and 1.9 mm, which agrees with the previously reported relative pose accuracy of 1.7° and 2.6 mm (Zuffi et al., 1999, for a single relative pose). Mahfouz et al. (2003) reported smaller errors (within 0.3° in rotation and 1.1 mm in translation), as did Banks and Hodge (1996) (within 1° and 1 mm); however these studies reported different error measures compared to the current study, which defined error as the difference in relative kinematics between the methods, determined over a range of relative poses between the implant components. In contrast, previous studies calculated the error for a single relative pose between the implant components (Banks and Hodge, 1996; Zuffi et al., 1999) or as a series of Euler angles from an error matrix (Mahfouz et al., 2003). The reported accuracy (Mahfouz et al., 2003) therefore represented the pose of the optoelectronically located femur in the coordinate system of the fluoroscopically located femur, and

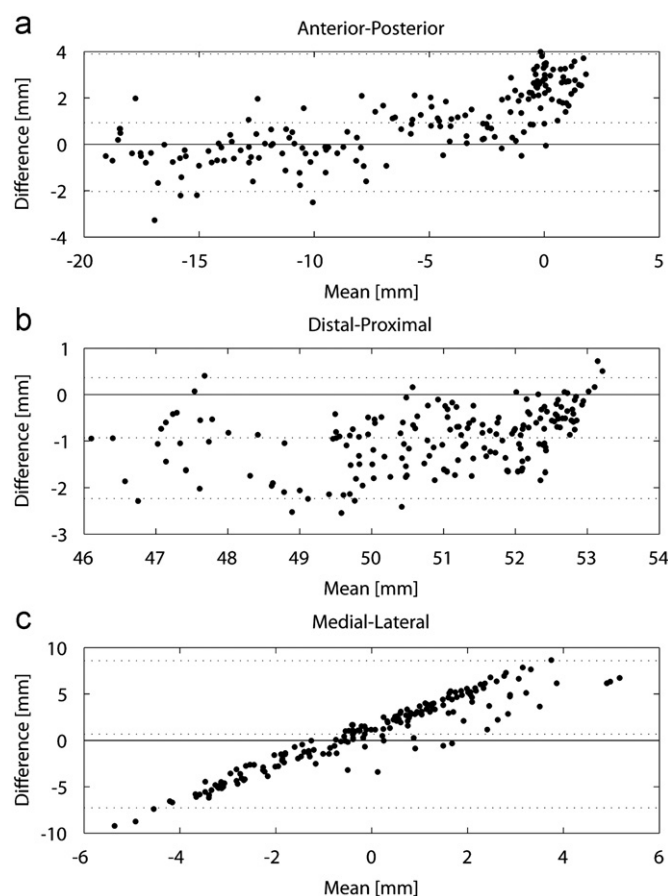


Fig. 4. Bland–Altman plots indicating the agreement between the two methods in determining relative knee joint translations during dynamic trials. For each pair of observations (one for the fluoroscopic method and one for the optoelectronic method), one point is plotted at the mean (horizontal axis) of the two observations and the difference (vertical axis) of the two observations. One Bland–Altman figure is plotted for each of the translation axes: (a) anterior–posterior, (b) distal–proximal, and (c) medial–lateral. The centre dotted line is plotted at the mean difference between the two methods. The upper and lower dotted lines are the limits of agreement, between which 95% of differences between the two methods are expected to fall.

could not be used as a measure of accuracy in determining the femur pose with respect to the tibia (knee joint kinematics).

The widest limits of agreement and the least repeatability were for medial–lateral translation, which was the direction perpendicular to the image plane. Although the size of the component silhouette changed as it was translated in the medial–lateral direction, the changes were subtle. Frontal (Fig. 2g) and axial (Fig. 2i) views of the components were helpful in determining a reasonable range of medial–lateral translation between the two components. Out-of-plane position estimates can be significantly improved using collision detection, which involves ensuring that the femoral component does not intersect with the polyethylene tibial insert (Hirokawa et al., 2008; Prins et al., 2010). The pose of the insert can be determined based on the tibial tray pose if a fixed bearing implant is used or based on beads embedded in the insert (Fantozzi et al., 2004). However, a mobile bearing implant with no beads was used in this study.

While this study provides a guideline for the accuracy of the fluoroscopic shape matching technique using this software, it is limited in that this study focused on only one joint (the knee) and used only one total knee replacement design. In addition, this study used Sawbones, which can be considered a “best case scenario”. In the study of human subjects, the contrast between the implant, cement, bone and soft tissues may not be as clear.

Finally, uncertainty in the optoelectronic data (locating components, digitizing landmarks) would have contributed to the

differences between the methods (Table 2). An individual infrared marker can be located to within 0.15 mm (Northern Digital Inc., Waterloo, Ontario, Canada). During the static trials, the standard deviations of the optoelectronically determined angles and translations of the femur with respect to the tibia were less than 0.008° and 0.02 mm, respectively. This variation is at minimum an order of magnitude smaller than the variation in differences between the two methods for the same static trials, indicating that optoelectronic contributions to uncertainty in determining knee joint kinematics were negligible.

The mean differences between the fluoroscopic and optoelectronic poses and the corresponding limits of agreement determined in this study reflect the accuracy with which the relative pose between knee replacement components can be determined by shape-matching single-plane fluoroscopic images and then using an automated optimization algorithm to optimize the match. The mean accuracy values and limits of agreement can be used to determine whether the shape-matching approach using single-plane fluoroscopic images is sufficient for an intended motion tracking application.

Conflict of interest statement

The authors have no conflicts of interest that would inappropriately influence the work in this study.

Acknowledgments

The authors gratefully acknowledge Maarten Beek for programming the data collection software to synchronize fluoroscopic image acquisition and infrared marker position tracking. This study was partially funded by the Natural Sciences and Engineering Research Council of Canada, the Human Mobility Research Centre at Queen's University/Kingston General Hospital, and Zimmer Inc., Warsaw, Indiana.

References

- Altman, D.G., Bland, J.M., 1983. Measurement in medicine – the analysis of method comparison studies. *Statistician* 32, 307–317.
- Banks, S.A., Hodge, W.A., 1996. Accurate measurement of three-dimensional knee replacement kinematics using single-plane fluoroscopy. *IEEE Transactions on Bio-medical Engineering* 43, 638–649.
- Bland, J.M., Altman, D.G., 1999. Measuring agreement in method comparison studies. *Statistical Methods in Medical Research* 8, 135–160.
- Bland, J.M., Altman, D.G., 2007. Agreement between methods of measurement with multiple observations per individual. *Journal of Biopharmaceutical Statistics* 17, 571–582.
- Canny, J., 1986. A computational approach to edge-detection. *IEEE Transactions on Pattern Analysis and Machine Intelligence* 8, 679–698.
- Fantozzi, S., Leardini, A., Banks, S.A., Marcacci, M., Giannini, S., Catani, F., 2004. Dynamic in-vivo tibio-femoral and bearing motions in mobile bearing knee arthroplasty. *Knee Surgery Sports Traumatology Arthroscopy* 12, 144–151.
- Grood, E.S., Suntay, W.J., 1983. A joint coordinate system for the clinical description of three-dimensional motions: application to the knee. *Journal of Biomechanical Engineering* 105, 136–144.
- Hirokawa, S., Hossain, M.A., Kihara, Y., Ariyoshi, S., 2008. A 3D kinematic estimation of knee prosthesis using X-ray projection images: clinical assessment of the improved algorithm for fluoroscopy images. *Medical & Biological Engineering & Computing* 46, 1253–1262.
- Mahfouz, M.R., Hoff, W.A., Komistek, R.D., Dennis, D.A., 2003. A robust method for registration of three-dimensional knee implant models to two-dimensional fluoroscopy images. *IEEE Transactions on Medical Imaging* 22, 1561–1574.
- Prins, A.H., Kaptein, B.L., Stoel, B.C., Reiber, J.H.C., Valstar, E.R., 2010. Detecting femur–insert collisions to improve precision of fluoroscopic knee arthroplasty analysis. *Journal of Biomechanics* 43, 694–700.
- Yamazaki, T., Watanabe, T., Nakajima, Y., Sugamoto, K., Tomita, T., Yoshikawa, H., Tamura, S., 2004. Improvement of depth position in 2-D/3-D registration of knee implants using single-plane fluoroscopy. *IEEE Transactions on Medical Imaging* 23, 602–612.
- Zuffi, S., Leardini, A., Catani, F., Fantozzi, S., Cappello, A., 1999. A model-based method for the reconstruction of total knee replacement kinematics. *IEEE Transactions on Medical Imaging* 18, 981–991.